

### **3. The ElarmS Earthquake Early Warning Methodology and Application across California**

**Richard M. Allen**

University of California Berkeley

In "Earthquake Early Warning Systems", P. Gasparini, G. Manfredi, J. Zschau (Eds), p. 21-44, Springer, ISBN-13 978-3-540-72240-3, 2007.

#### **Abstract**

Earthquake Alarms Systems, ElarmS, is a methodology for providing warning of forthcoming ground shaking during earthquakes. The approach uses a network of seismic instruments to detect the first-arriving energy at the surface, the P-waves, and translate the information contained in these low amplitude waves into a prediction of the peak ground shaking that follows. The instruments closest to the epicenter are the first to detect the seismic energy, and by using a seismic network this information can be integrated to produce a map of future ground shaking everywhere. The ElarmS methodology uses the frequency content of the P-wave arrival to estimate earthquake magnitude, arrival times to determine location, and then predicts the ground shaking using a radial attenuation relation. All data is gathered continuously and the hazard map updated every second. As observations of peak ground shaking are also made close to the epicenter they are integrated into the hazard assessment. Here, the methodology is applied to a set of 32 earthquakes in southern California to assess the accuracy and timeliness of warning if such a system was implemented using the existing seismic network. If there was no data telemetry delays the first warning would be available before the S-wave arrival at the epicenter for 56% of the earthquakes. The average absolute magnitude error at this time is 0.44 units and the error in the average absolute peak ground acceleration [ $\ln(\text{PGA}_{\text{predicted}}) - \ln(\text{PGA}_{\text{observed}})$ ] is 1.08. Within 5 sec warning are available for 97% of the events, the average magnitude error is 0.33 units, and the average PGA error is 1.00. To further assess the utility of ElarmS implementation in California, probabilistic warning time distribution functions are determined for cities in northern California. Using the set of future likely earthquakes provided by the Working Group on California Earthquake Probabilities (2003) the warning times that the ElarmS methodology could provide (if implemented) can be estimated, and a probability of occurrence associated.

The alarm time is defined as the time when 4 sec of P-wave data is available at 4 seismic stations. At this point in time the average magnitude error is 0.5 units. The warning times range from zero seconds to over a minute, the most likely warning times range from seconds to a few tens of seconds depending on location. The largest magnitude earthquakes are also associated with the greatest warning times and it is more likely than not, that San Francisco would receive more than 20 sec warning for earthquakes generating the most damaging ground shaking.

## **3 The ElarmS Earthquake Early Warning Methodology and Application across California**

Richard M. Allen

University of California Berkeley

### **3.1 Introduction**

Current earthquake mitigation in the United States focuses on long-term characterization of the likely levels of ground shaking and the frequency of occurrence (e.g. Frankel et al. 1996). These estimates are the basis for building codes which aim to prevent collapse during earthquakes. The approach is highly effective at reducing deaths but not necessarily at reducing the cost of earthquakes. While buildings may not collapse during an earthquake, they may still suffer structural damage requiring them to be demolished. In other countries, including Mexico, Japan, Taiwan and Turkey, earthquake warning systems (EWS) are used in addition to building codes to further reduce the impact of earthquakes (Espinosa Aranda et al. 1995; Wu et al. 1998; Wu and Teng 2002; Erdik et al. 2003; Odaka et al. 2003; Boese et al. 2004; Kamigaichi 2004; Nakamura 2004; Horiuchi et al. 2005; Wu and Kanamori 2005). Short-term mitigation actions are taken in these countries to reduce both financial losses and casualties.

Earthquake warning systems (EWS) rapidly detect the initiation of earthquakes and warn of the forthcoming ground shaking. For a specific city, such as San Francisco, the warning time could be tens of seconds for some earthquakes, while zero seconds for others. However, in situations when San Francisco gets zero seconds warning, surrounding cities such as Oakland would likely get a few seconds and San Jose would get ~15 sec warning. Thus, for any earthquake scenario in a densely populated region, such as the San Francisco Bay Area (SFBA) or the Los Angeles Metropolitan Area (LAMA), an EWS could provide warning to at least some of the affected population in a damaging earthquake.

Here we present one methodology for an EWS that could be implemented in California and other regions around the world. The Earthquake Alarm System, “ElarmS,” is designed to predict the distribution of peak ground shaking across the region affected by an earthquake before the beginning of significant ground motion (see <http://www.ElarmS.org>). ElarmS

uses the first few seconds of P-wave arrivals at the closest stations to the epicenter to locate an earthquake and estimate its magnitude. A map—AlertMap—of predicted ground shaking is then generated and updated as more information becomes available. We apply the methodology to the specific problem of earthquake warning in southern and northern California using datasets of past and likely future earthquakes. In southern California, we use a set of past earthquakes and apply the methodology to determine the accuracy of the warnings generated. In northern California, we estimate the warning times that would be available for locations across the SFBA for all likely future earthquakes identified by the Working Group on California Earthquake Probabilities (2003).

### **3.2 The ElarmS Methodology**

The ElarmS methodology was designed with the goal of predicting the distribution of peak ground shaking across the region affected by an earthquake before the beginning of significant ground motion at the epicenter. The first few seconds of the P-wave at the station and stations closest to the epicenter is used to estimate the magnitude of the earthquake and attenuation relations provide the predicted distribution of ground shaking as a function of distance from the epicenter. The complete ElarmS system is designed to generate a map of predicted peak ground shaking, a predicted-ShakeMap that we call “AlertMap.” The first AlertMap is available 1 sec after the first P-wave trigger and is updated every second as additional data is gathered from stations farther from the epicenter. Below, we describe the three components of ElarmS.

#### **3.2.1 Earthquake location and warning time estimation**

Earthquakes are located using the arrival times of P-waves. When the first station triggers, an event is located at that station with a depth typical of events in the region. The earthquake is then located between the first two, and then the first three, stations to trigger. Once four stations have triggered a grid search method is used to locate the event, minimizing the misfit between predicted and observed arrival times.

The warning time is defined as the remaining time until the onset of peak ground shaking and can be estimated given the origin time and location of the earthquake using S-wave arrival time curves. The use of the predicted S-arrival time provides a conservative estimate of the remaining warning time. In larger magnitude earthquakes, such as Northridge and

Loma Prieta, peak ground shaking occurred 5-10 sec after the S-arrival at stations tens of kilometers from the epicenter.

### 3.2.2 Rapid earthquake magnitude estimation

The magnitude of an earthquake is rapidly estimated using the frequency content of the first four seconds of the P-wave arrival. The predominant period,  $\tau_p$ , of the vertical component waveform is calculated using the method first described by Nakamura (1988), and the maximum value within 4 sec,  $\tau_p^{\max}$ , is found to scale with event magnitude (Allen and Kanamori 2003; Lockman and Allen 2005; Olson and Allen 2005; Lockman and Allen 2007). Before calculation of  $\tau_p$ , accelerometer recordings are converted to velocity and all processing is done recursively in a causal fashion.  $\tau_p$  is determined continually in realtime from the vertical component velocity waveform using the relation

$$\tau_i^p = 2\pi\sqrt{X_i/D_i} \quad (3.1)$$

where

$$X_i = \alpha X_{i-1} + x_i^2 \quad (3.2)$$

$$D_i = \alpha D_{i-1} + \left(\frac{dx}{dt}\right)_i^2 \quad (3.3)$$

$x_i$  is the ground motion recorded at time  $i$  and  $\alpha$  is a 1 sec smoothing constant (for 100 sps data  $\alpha=0.99$ , for 20 sps data  $\alpha=0.95$ ). The higher frequency content of smaller magnitude earthquakes is measurable within a shorter time period after the P-wave arrival than the low frequency energy of larger events. Correspondingly, the magnitude of smaller events can be determined more rapidly than that of larger events. This also means that the magnitude estimate after 1 s is a minimum estimate, and once 2, 3 and 4 s of data are available, the magnitude estimate may increase.

Two linear relations between  $\tau_p^{\max}$  and magnitude are used (Allen and Kanamori 2003). For smaller earthquakes (magnitudes 3.0 to 5.0), broadband data low-pass filtered at 10 Hz is used and a good magnitude estimate is possible given just 1 s of data. With 2 s of data the magnitude error reduces slightly, but additional data does not improve the estimate. Using

our  $\tau_p^{\max}$  observations from the broadband waveforms after 2 s and minimizing the average absolute deviation we determine the relation

$$m_l = 6.3 \log(\tau_p^{\max}) + 7.1 \quad (3.4)$$

to estimate the magnitude of low-magnitude earthquakes. For larger magnitude events (magnitude  $> 4.5$ ), better estimates are possible with the application of a 3 Hz low-pass filter and the best estimates of magnitude require 4 s of data, although minimum magnitude estimates can be made as soon as 1, 2 and 3 s after the P-arrival. The best-fit high-magnitude relation is

$$m_h = 7.0 \log(\tau_p^{\max}) + 5.9. \quad (3.5)$$

Both  $m_l$  and  $m_h$  are used by ElarmS to produce the best estimate of magnitude. Initially, 1 sec after a station triggers,  $m_l$  is calculated from  $\tau_p^{\max}$ , and when 2 s of data are available the estimate is updated. Station-magnitude estimates (one from each triggered station) are averaged to provide an event-magnitude estimate. If the event-magnitude estimate becomes greater than 4.0, then  $m_h$  is also calculated and the event-magnitude estimate is the average of both  $m_l$  and  $m_h$  from each triggered station.

$\tau_p^{\max}$  has been calculated for earthquakes with magnitudes ranging from 3.0 to 8.3 from various regions around the world (Fig. 3.1). Datasets with a wide magnitude range from southern California and Japan show a similar scaling relation between the value of  $\tau_p^{\max}$  and magnitude (Allen and Kanamori 2003; Lockman and Allen 2007), and a global dataset including waveforms from southern California, Japan, Taiwan and the Denali earthquake in Alaska suggest that the scaling relation does not break down for even the largest magnitude earthquakes (Olson and Allen, 2005).

The accuracy of magnitude estimates is a function of the number of stations providing P-wave data. Figure 3.2 shows how the average error of magnitude estimates decreases as  $\tau_p^{\max}$  observations at multiple stations are combined to provide an average magnitude estimate. Datasets from southern California and Japan show a similar relation. Using just the closest station to the epicenter the average magnitude error is  $\sim 0.75$  magnitude units; once data from the closest 2 stations is available the error drops to  $\sim 0.6$ , and to  $\sim 0.5$  magnitude once 4 stations provide data.

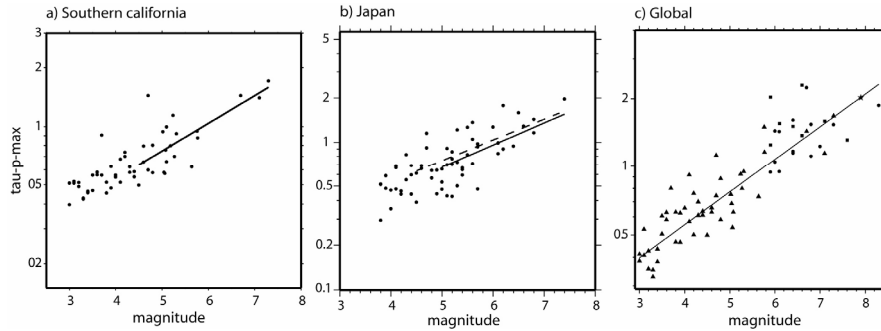


**Fig. 3.1** Scaling relation between event-averaged  $\tau_p^{\max}$  and magnitude. All data has been processed using the same recursive algorithms. **A)** Southern California earthquakes and best fit relation (solid line). **B)** Earthquakes in Japan and best fit relation (solid line). The dashed line is the best fit relation for California shown in A, which is nearly identical. **C)** Global compilation of earthquakes including southern California, Japan, Taiwan and the Denali earthquake. Waveforms are a mixture of accelerometers and broadband velocity instruments.

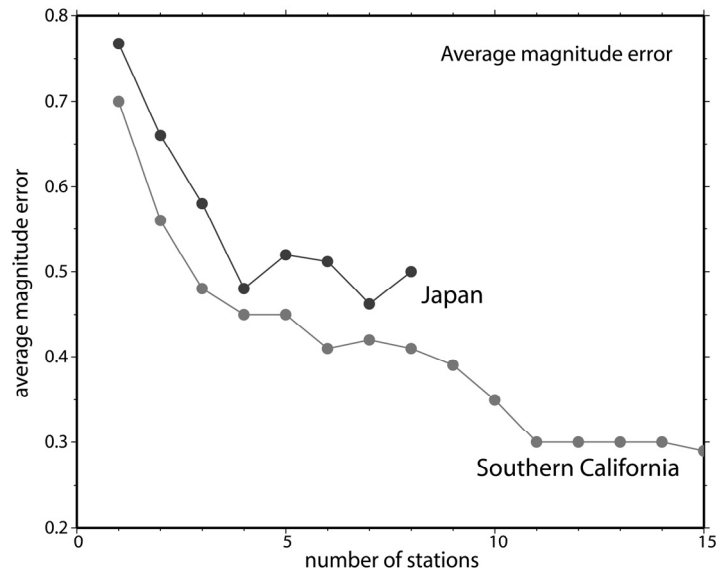


**Fig. 3.2** Average absolute error in magnitude estimates as a function of the number of stations providing P-wave data for all events studied in southern California (green) and Japan (red). Using 1 station, the average error is  $\sim 0.75$  magnitude units, and drops to  $\sim 0.6$  with 2 stations and  $\sim 0.5$  once 4 stations provide data.

### 3.2.3 Predicting the distribution of ground shaking

Given the location and magnitude of an earthquake, the spatial distribution of peak ground shaking can be estimated using attenuation relations. Most existing relations use only ground motion observations for earthquakes with magnitudes greater than 5.0. ElarmS uses its own attenuation relations developed from regional observations for events with magnitudes greater than 3.0. Designing ElarmS to be operational during the frequent low magnitude events as well as large events is desirable in order to continually test the system.

Many different functional forms have been used for different types of earthquakes in different regions (e.g. Campbell 1981; Joyner and Boore 1981; Fukushima and Irikura 1982; Abrahamson and Silva 1997; Boore et al. 1997; Campbell 1997; Sadigh et al. 1997; Field 2000), however most are based on the functional form

$$A = A_0 r^n e^{-kr} \quad (3.6)$$

where  $A$  is the peak ground acceleration (PGA) at a distance  $r$ , and  $A_0$ ,  $n$  and  $k$  are constants to be determined. This functional form has a term for geometric spreading,  $r^n$ , and one for intrinsic attenuation,  $e^{-kr}$ . Using a dataset of local earthquakes ranging in magnitude from 3.0 to 7.3 from southern California, best-fit attenuation relations were determined for the region. The effect of intrinsic attenuation was not significant within 200 km of an event, so  $k$  was set to zero to reduce the unknowns in the regression.  $n$  was determined as a function of magnitude by grouping PGA observations by magnitude and calculating the best fitting  $n$ . Having determined  $n$ ,  $A_0$  was calculated for each event and the best fitting linear relation between  $A_0$  and magnitude was obtained. Figure 3.3 shows how  $A_0$  and  $n$  vary as a function magnitude.

ElarmS uses the attenuation relations in a two-stage process. One second after the first P-wave trigger the first estimate of magnitude is available. Given the magnitude,  $A_0$  and  $n$  are determined from the relations shown in Fig. 3.3, and estimated PGA is calculated as a function of distance. As time progresses during the event sequence, the stations closest to the epicenter measure their PGA. Once this information is available from a few stations, it is used to adjust the attenuation relation by keeping  $n$  fixed but allowing  $A_0$  to change in order to best-fit the attenuation relation to PGA observations. Figure 3.4 shows examples of the attenuation relations for several earthquakes. Note the discrepancy between the observations and predictions of the Field (2000) attenuation relations. This discrepancy is a common problem when using attenuation relations determined from

larger-magnitude events only. The attenuation relations described here do not account for near-surface amplification effects, such as rock versus soil, which are responsible for much of the scatter in the acceleration observations shown in Fig. 3.4. Although site corrections are not currently part of ElarmS, they can easily be included when known (e.g. Wald et al. 1999; Wald et al. 1999).

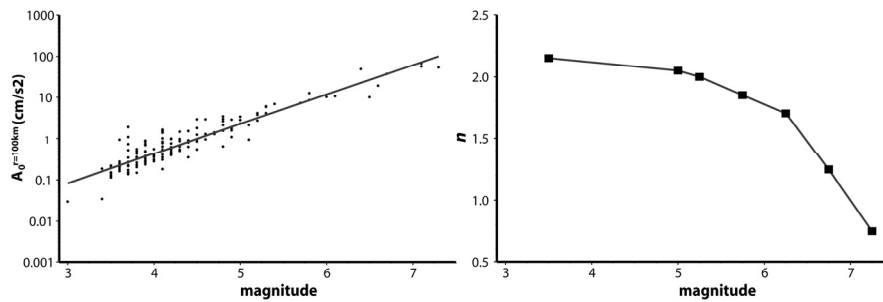


**Fig. 3.3** Empirically determined values of  $n$  and  $A_0$  as a function of earthquake magnitude. PGA observations were initially grouped by magnitude and  $n$  determined for each group by regression. Having determined  $n$ , the best fitting  $A_0$  (defined as the amplitude at  $r=100$  km) was calculated for each event. Linear regression provides  $A_0$  as a function of magnitude.

### 3.3 Accuracy and timeliness of warnings

To test the accuracy and timeliness of warning information we gather a dataset of 32 earthquakes from southern California. The events were selected to give as wide a range of magnitude as possible and to include the events occurring beneath the denser portions of the existing broadband network. Earthquakes with magnitude ranging from 3.0 to 5.4 were included as shown in Fig. 3.5. All events with magnitudes larger than 5.4 either occurred before the existing seismic network was in place (e.g. Landers and Northridge), or were in locations where the network is sparse (e.g. Hector Mine).

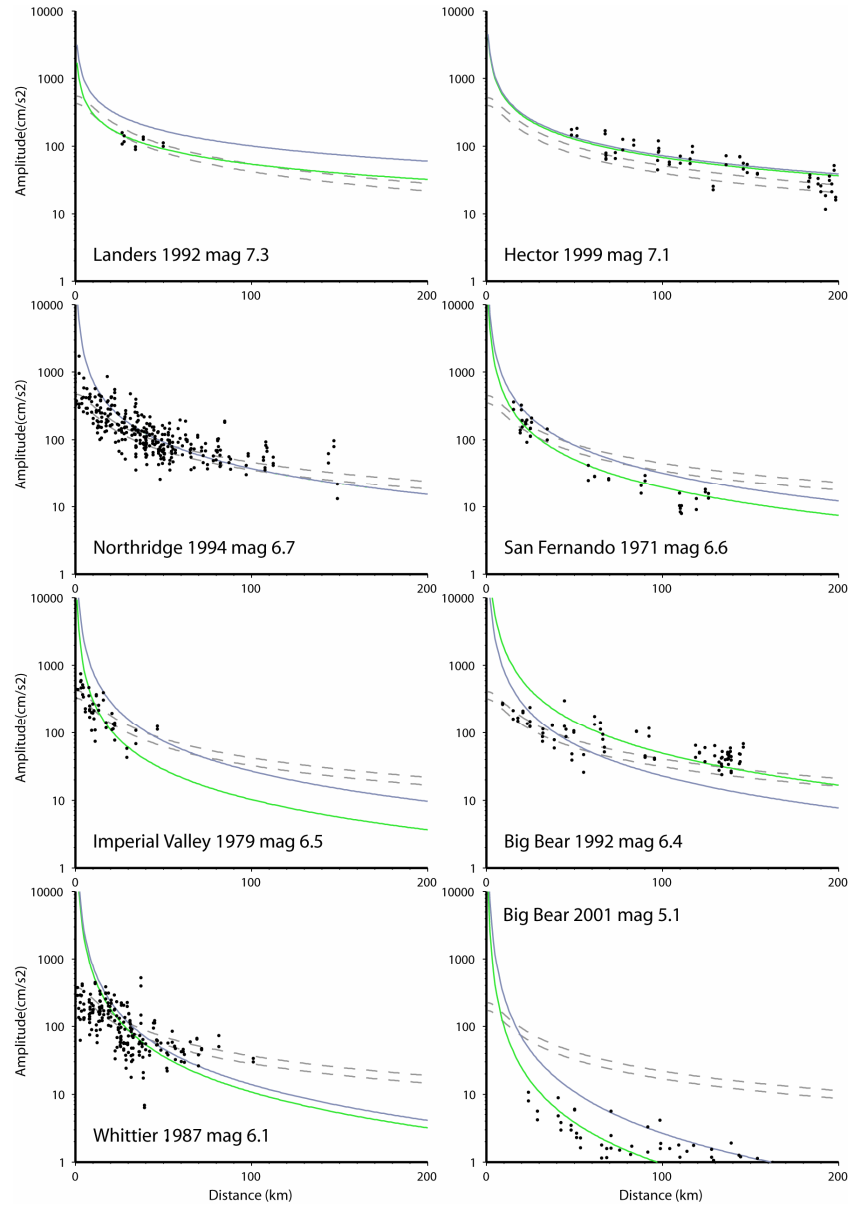


**Fig. 3.4** Examples of attenuation relations (lines) and PGA observation (dots) for eight southern California earthquakes with magnitudes ranging from 5.1 to 7.3. Grey lines show the ElarmS attenuation relations determined given just earthquake magnitude and the green lines are the result of adjusting the relation based on PGA observations. Dashed lines show the Field (2000) attenuation relations for rock and soil for comparison.

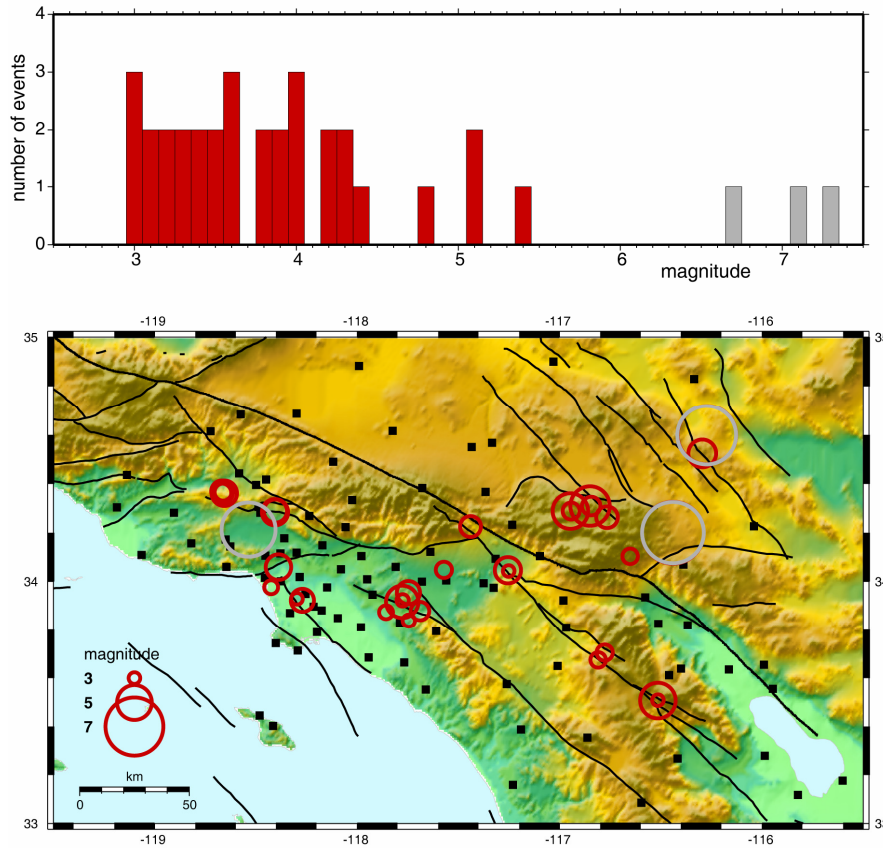


**Fig. 3.5** Map of southern California showing the 32 earthquakes used to assess the accuracy and timeliness of ground shaking warnings. The 32 events occurred beneath the denser portions of the seismic network in the regions which are also the most densely populated. The histogram shows the magnitude distribution of the events included (red). The three largest magnitude events (grey on map and histogram) were not included as they did not occur beneath the current dense array.

The waveform datasets from these events are processed using the ElarmS methodology to determine the magnitude and the predicted ground shaking (PGA) as a function of time. We find that initial magnitude and PGA estimates are available for 56% of the earthquakes by the time the S-wave arrived at the surface, Fig. 3.6. We use the S-arrival at the epicenter as the zero time, because this is the earliest possible time of peak ground shaking at the surface, although in large magnitude earthquakes the peak

ground shaking typically occurs 5 to 10 sec after the S-wave arrival at local sites. This test does not include any delays in data transmission, which would delay warnings by 1 or 2 sec, depending on how the early warning algorithms are implemented. Note, however, that likely telemetry delays are less than peak ground shaking delays for large magnitude earthquakes. With no telemetry delay and peak ground shaking at the time of the S-wave arrival, warnings would be available for more than 50% of earthquakes at the epicenter. If there is a 2 sec telemetry delay, then warning would be available for more than 50% of earthquakes at locations greater than ~8 km from the epicenter. This “blind zone” close to the epicenter, where warning may not be available using ElarmS, is also the region where some of the most severe damage would likely occur. Single station approaches to onsite early warning can offer timely hazard information in these regions (e.g. Nakamura 1996, 2004; Lockman and Allen 2005; Wu and Kanamori 2005; Wu and Kanamori 2005; Wu et al. in review). It should also be noted that, although the intensity of ground shaking may be lower outside the blind-zone than within, the total hazard exposure outside the blind-zone may be greater than within it. For example, buildings were red-tagged as structurally unsafe and scheduled for demolition as far as 60 km from the epicenter in the 1994 Northridge earthquake in LAMA. In that event, an 8 km radius blind-zone represented less than 2% of the total area severely affected by the earthquake.

While the first hazard prediction is available 1 sec after the first P-wave arrival, the majority of the initial predictions in Fig. 3.6 are based on trigger times and magnitude estimates from more than one seismic station. The offline algorithms used in this test gather all available information and update hazard estimates once per second. The density of seismic stations (typically 20 km spacing in the populated regions) means that, within a 1 sec time interval, usually two, and often three, stations trigger. The first event location, hazard, and warning time estimates, therefore, are based on information from multiple stations, providing a more accurate location and magnitude estimate than using a single station.

The test shows that magnitude estimates are available for 56% of earthquakes at the time of the S-arrival with an average magnitude error of 0.44 magnitude units, Fig. 3.6A. Within 5 sec, magnitude estimates are available for 97% of events and the average error is down to 0.33 magnitude units. Figure 3.6B shows the error in the PGA estimates as a function of time. PGA is estimated at each station within 100 km of the event using the available ElarmS magnitude and location and the attenuations relations described above. The error in the PGA estimate is calculated in the usual way: it is the natural logarithm of the predicted PGA minus the natural logarithm of the observed PGA for the event. At the time of the S-arrival,

the average absolute error is 1.08. It drops to 1.00 within 5 sec, 0.98 within 10 sec, and reaches 0.95 at 15 sec. When the correct magnitude is used in the attenuation relations (thus removing the error in the ElarmS magnitude estimate), the error is only slightly lower: 0.89. An error in PGA of 1 is equivalent to the difference between a Modified Mercalli Intensity (MMI) of IV to V or alternatively of VIII to X.

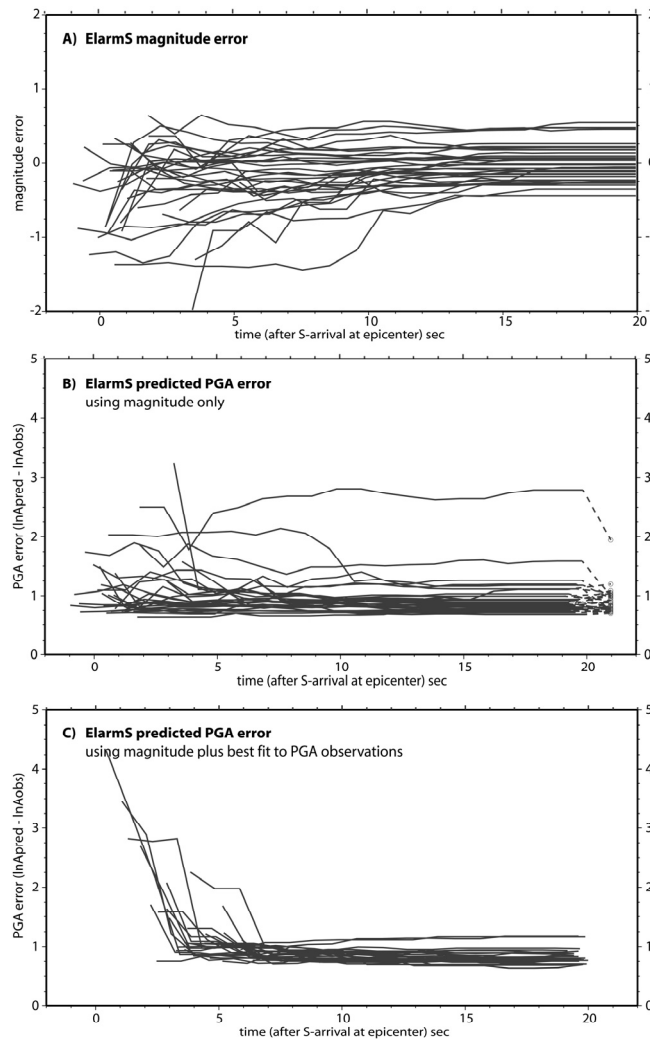


**Fig. 3.6** The results of testing ElarmS offline using a set of 32 earthquakes in southern California designed to assess the accuracy and timeliness of warning information given the current distribution of stations. All panels show errors as a function of time with respect to the S-wave arrival at the epicenter, which repre-

sents the earliest time of peak ground shaking during an earthquake. **A)** The error in the magnitude estimate. **B)** Average absolute error in PGA estimates at all stations using available magnitude and location estimates and the ElarmS attenuation relations. The open circles at the far right are the errors when the true magnitude is used. **C)** Average error in PGA once available PGA observations are incorporated. The error in the PGA estimates is calculated in the usual way: the error is the natural logarithm of the predicted PGA minus the natural logarithm of the observed PGA for the event.

As time progresses during an earthquake, the closest stations record their PGA and this information is included in the prediction for stations at greater distances from the epicenter. The error in the PGA prediction once PGA observations from near stations are incorporated, is shown in Fig. 3.6C. At 5 sec, the average error is 1.02, similar to when PGA observations are not included, but it drops to 0.85 at 10 sec and 0.82 at 15 sec, which is slightly better than just using magnitude estimates alone. The most important use of PGA observations is to remove outliers, that is, cases when the magnitude-based estimate is very high or low.

### **3.4 Warning time distributions for northern California**

Having assessed the timeliness and accuracy of warnings in southern California, we look to the likely distribution of warning times in northern California should the ElarmS methodology be implemented using the existing seismic network. We use the set of likely earthquake scenarios for northern California identified by the Working Group on California Earthquake Probabilities (2003). Each earthquake scenario has an associated probability of occurrence by the year 2032, allowing determination of probabilistic warning time distributions for any location in the region.

To calculate the warning times, we define an “alert time” intended to represent the time when sufficient information about an earthquake is available for users to take action. During any earthquake the accuracy of warning information will increase with time and specific users will define the certainty level required for their own mitigation action (Grasso and Allen in review). Here, we choose a single threshold based on the accuracy of the warning and use the point in time when 4 sec of P-wave data are available at four seismic stations. This is defined as the alert time and represents the time when the average error in the magnitude estimate will be  $\sim 0.5$  magnitude units based on tests in southern California and Japan (see Fig. 3.2). The warning time is the difference between the alert time and the

estimated time of peak ground shaking for a given location. For the arrival-time of peak ground shaking as a function of epicentral distance we use the S-wave arrival-time curve out to a distance of 150 km and then a constant moveout of 3.55 km/s based on the observed moveout of peak ground shaking in California.

Warning times are calculated for a total of 4070 earthquake epicenters. These epicenters were distributed at 1 km intervals along the faults identified as those most likely to cause damaging earthquakes in northern California by the Working Group on California Earthquake Probabilities (2003). The study identified seven fault systems, each of which has one or more rupture segments, as shown in Fig. 3.7, that can rupture on their own or with adjacent segments. In all, 35 earthquake rupture scenarios were identified and a probability of occurrence within 30 years was estimated for each. The total probability of one or more of these earthquake scenarios (with magnitudes ranging from 5.8 to 7.9) occurring before 2032 is 84%. Within the SFBA, the faults that are most likely to rupture are the San Andreas Fault and the Hayward-Rodgers Creek Fault with probabilities of producing a magnitude 6.7 or greater earthquake of 21% and 27% respectively. The aggregate probability of one or more magnitude 6.7 or greater earthquakes within the next 30 years (from 2003 to 2032) in the SFBA is 62%.

Each of these earthquake scenarios involves rupture across a finite fault plane. The warning time in a given earthquake is dependent on the epicentral location where the rupture initiates. We do not know the likely point of initiation for the 35 scenarios; therefore, we accommodate the uncertainty in epicentral location by distributing epicenters at 1 km intervals along each fault. The probability of an earthquake with each epicentral location within one rupture scenario is set equal, and the aggregate probability of all the epicenters is equal to the scenario probability.

Given the epicenter of an earthquake, the alert time is dependent on the relative locations of seismic stations to detect the P-wave arrivals. Several thousand seismic stations are operated in northern California by the California Integrated Seismic Network (CISN), which consists of multiple, complementary seismic networks (see <http://www.cisn.org>). The ElarmS methodology requires continuous seismic waveforms recorded by instruments with a broad frequency sensitivity, i.e. continuous broadband stations. Such instruments are operated by the University of California Berkeley, which contributes a network of 24 stations, each with a broadband velocity seismometers and an accelerometer, and the U.S. Geological Survey, which operates approximately 100 accelerometers, located mostly in the SFBA, and 15 broadband velocity seismometers. In total, there are ap-

proximately 140 seismic stations across northern California which could be used in an EWS, Fig. 3.7.

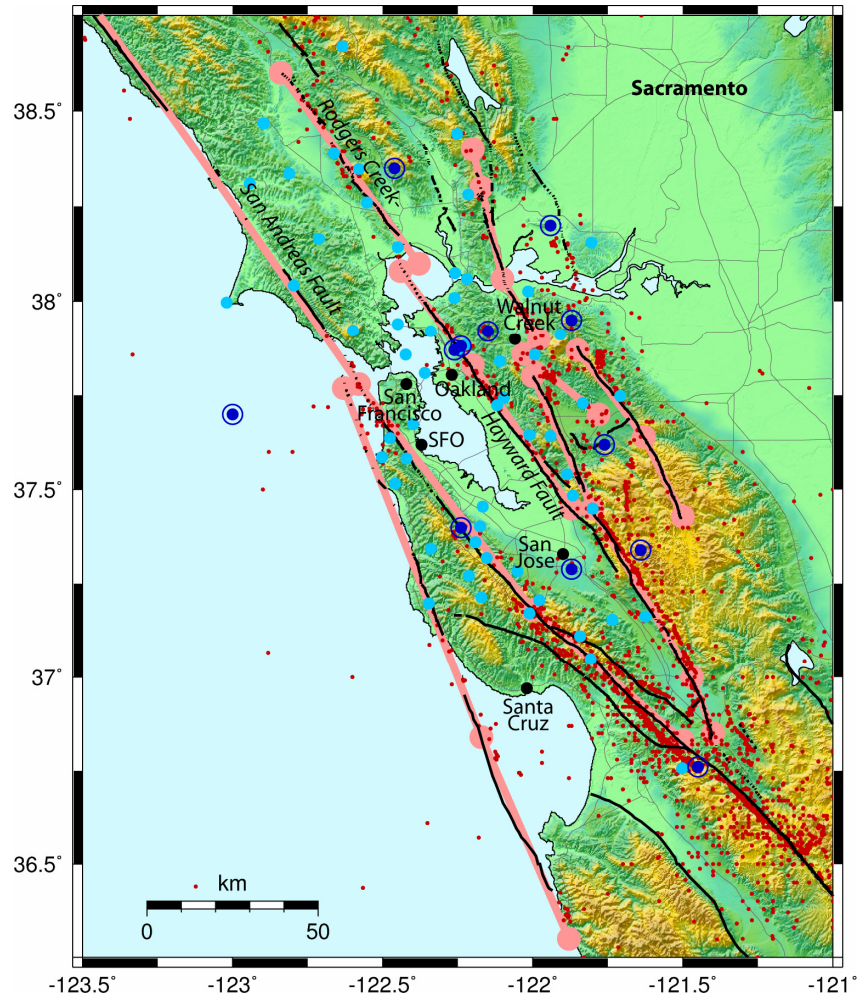


**Fig. 3.7** Map of the San Francisco Bay Area (SFBA) showing mapped faults (bold black lines) and the location of earthquakes with magnitude greater than 3 since recording began (red dots). Existing continuous broadband stations operated by UC Berkeley (dark blue) and the U.S. Geological Survey (light blue) are shown with circles for broadband velocity seismometers and dots for accelerometers. The fault segments identified by the Working Group on California Earthquake Probabilities (2003) are shown with pink dots at the ends of segments joined by broad pink lines. The six “warning points” included in Figs 3.8 and 3.9 are shown as black dots.

The alert time for each earthquake epicenter is calculated as the time at which 4 sec of P-wave data are available at the 4 closest continuous broadband stations plus a fixed telemetry and processing delay of 4.5 sec. A 4.5 sec delay accounts for transmission of waveform data from each station to one of the network operation centers, processing time, and transmission of the warning out to the user community. Given the current seismic infrastructure in northern California, the most significant delay is packetization of data before transmission from each station. We introduce a 2.5 sec delay for packetization, which represents the delay at the slowest existing stations. We add 1 sec for transmission to the processing center and 1 sec for transmission of the warning message. The processing time for the data is negligible. The warning time estimates, therefore, represent what is possible using the existing seismic network hardware. They could be improved through upgrade of telemetry and processing systems as well as the addition of seismic stations.

The warning time probability density function (WTPDF) for the city of San Francisco is shown in Fig. 3.8. This WTPDF is specifically for the Civic Center; however, it does not vary significantly over the rest of the city. For all the likely damaging earthquakes in the region, San Francisco could receive warnings varying from 77 sec down to -8 sec. Negative warning times mean no warning is possible. The most likely warning times are less than 25 sec; however, the WTPDF has a long tail which is due to the San Andreas Fault. In a repeat of the 1906 earthquake, a 450 km long segment of the fault could rupture. If the event nucleates off the Golden Gate, there would be little or no warning for San Francisco. However, assuming that it is equally likely that rupture nucleates anywhere along the fault, it is more likely that the epicenter is at a significant distance from San Francisco and there could be tens of seconds warning for this most damaging earthquake scenario. It should be noted that the 1906 rupture probably did nucleate off the Golden Gate (Bolt 1968; Boore 1977; Zoback et al. 1999; Lomax 2005). Whether this means that a future rupture would nucleate in the same location is unknown.

In addition to the warning times for each earthquake, we also estimate the likely intensity of ground shaking at the warning point, i.e. the Civic Center in the case of Fig. 3.8. These intensities are derived from Shake-Map scenario calculations (Working Group on California Earthquake Probabilities 2003). The grey regions in Fig. 3.8 represent earthquakes for which shaking intensity at the Civic Center is less than V on the MMI scale (Richter, 1958) and there is unlikely to be damage. Above a MMI V, the likely damage increases with the severity of shaking from light (V: unstable objects displaced), to strong (VII: broken furniture and damage to

masonry), to violent (IX: masonry seriously damaged or destroyed, frames displaced from foundations).

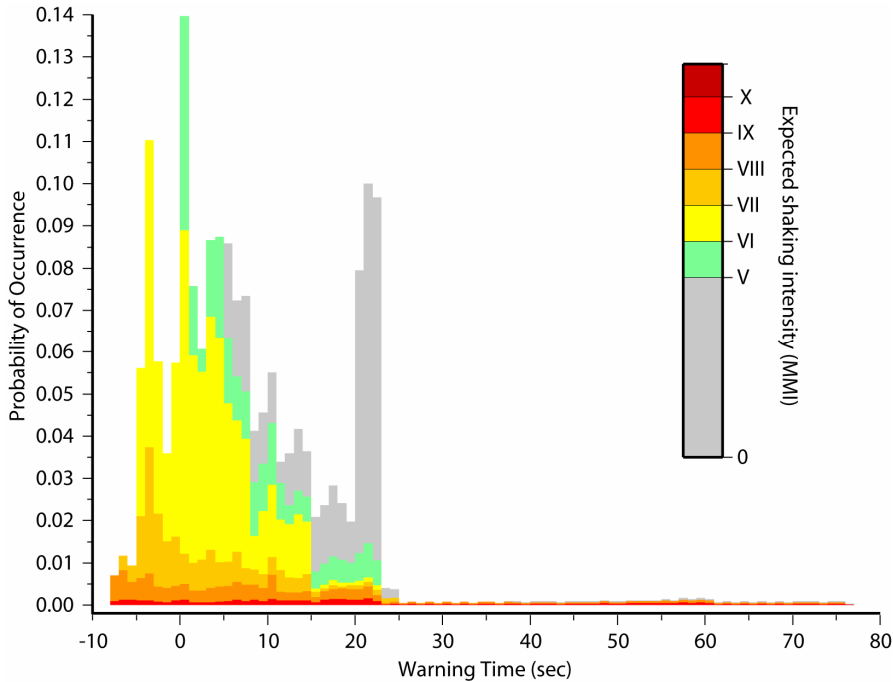


**Fig. 3.8** Warning time probability density function (WTPDF) for the Civic Center of San Francisco ( $37.78^{\circ}\text{N}$ ,  $122.42^{\circ}\text{W}$ ). The warning times for all likely earthquakes range from -8 sec to 77 sec, negative warning times mean no warning is possible. Earthquakes are in 1 sec bins and the vertical axis shows the total probability of one or more earthquakes occurring before 2032 with a given warning time. The color represents the estimated intensity of ground shaking for each event. Damage is unlikely for  $\text{MMI} < \text{V}$  (grey);  $\text{MMI} > \text{IX}$  means violent shaking likely to cause serious damage to buildings (red).

In the case of the WTPDF for San Francisco, Fig. 3.8, the long tail of large warning times includes a large portion of the earthquake scenarios which will cause violent ( $\text{MMI} > \text{IX}$ ) ground shaking. This is because the intensity of ground shaking in a given earthquake is dependent on the closest distance to the fault rupture, while the warning time is dependent on the distance to the epicenter. Our warning time estimates are conservative in that they represent the traveltime of shear energy directly from the epicenter to the warning point. The true time of peak ground shaking may not occur until the rupture has propagated along the fault to the closest point,

which is typically at less than the shear-wave speed, and then from the fault to the warning point at the shear-wave speed.

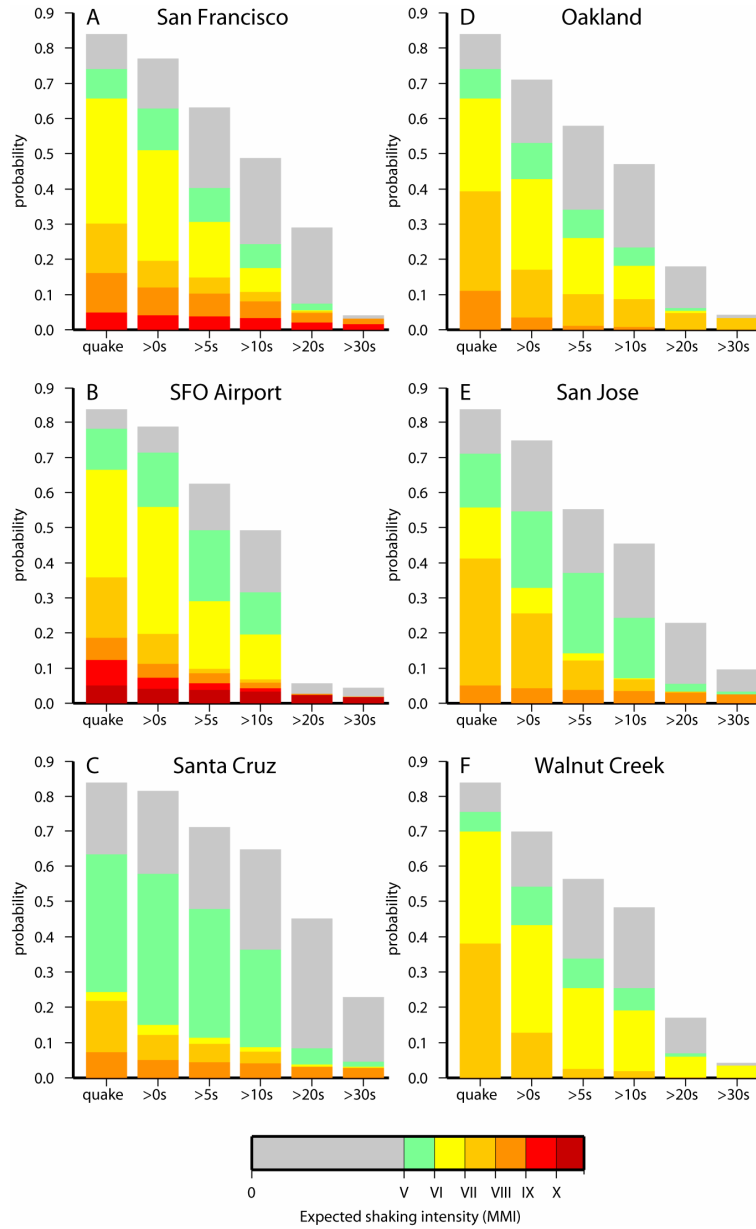


**Fig. 3.9** Simplified warning time probability density functions (WTPDF) for six locations around the SFBA. In each panel, the first column shows the aggregate

probability of all likely earthquakes in the region before 2032 (84%) and the expected intensity of ground shaking. The remaining columns show the probability of an earthquake occurring for which more than 0, 5, 10, 20 and 30 sec warning could be available, and the distribution of ground shaking intensities for those events. The six locations are shown on Fig. 3.7. **A)** The city of San Francisco (37.78°N, 122.42°W). **B)** San Francisco International Airport, SFO (37.62°N, 122.37°W). **C)** The city of Santa Cruz (36.97°N, 122.03°W). **D)** The city of Oakland (37.805°N, 122.270°W). **E)** The city of San Jose (37.33°N, 121.90°W). **F)** The city of Walnut Creek (37.90°N, 122.06°W).

Simplified representations of the WTPDF for six locations around the SFBA are shown in Fig. 3.9. The full WTPDF for these locations and other cities and sites of engineering interest are available at <http://www.ElarmS.org>. Figure 3.9A shows that there is a 74% probability of one or more earthquakes that will cause some damage ( $\text{MMI} \geq \text{V}$ ) in San Francisco by 2032, and a 63% probability of a damaging event for which a warning could be available. There is a 5% probability of an earthquake that causes violent ground shaking ( $\text{MMI} \geq \text{IX}$ ), and a 3% chance of one for which greater than 10 sec of warning could be available. It is therefore more likely than not that more than 10 sec warning would be available before violent ground shaking in the city. The WTPDF for the San Francisco International Airport (Fig. 3.9B) is similar to that for the city, except that the intensity of ground shaking could be greater given the closer proximity to the San Andreas Fault.

The most severe earthquakes for East Bay Cities occur on the Hayward-Rodgers Creek Fault. Its close proximity to cities such as Oakland (Fig. 3.7) make for reduced warning times, but also lower intensities due to the shorter length of the fault. It is still more likely than not that a warning will be available for a damaging earthquake, Fig. 3.9D. Most of the hazard for San Jose comes from the San Andreas Fault. As with San Francisco, this means there is a high probability of large warning times for the most damaging earthquakes. While there is a 5% probability of an event causing  $\text{MMI VIII}$  in San Jose, there is a 3% chance of an event for which there could be greater than 20 sec warning (Fig. 3.9E). In the October 17, 1989, Loma Prieta earthquake ( $M_w$  6.9), the closest city to the epicenter, Santa Cruz, experienced  $\text{MMI VIII}$ . There is a 7% probability of a similar intensity of ground shaking by 2032, and a 3% chance of similar ground shaking for which greater than 30 sec warning could be available (Fig. 3.9C). Finally, the rapidly growing urban areas east of the Berkeley Hills, such as Walnut Creek, are as likely to experience damaging ground shaking as San Francisco, although the most severe events have a lower intensity (Fig.

3.9F). As is the case for all locations in the SFBA, Walnut Creek could receive a warning before ground shaking starts for the majority of damaging earthquakes.

### **3.5 Earthquake warning outlook**

An EWS for San Francisco was first suggested by Cooper (1868), who proposed that the telegraph cables radiating from the city could transmit warning ahead of ground shaking. He also noted that this would not work if the center of the “shock” was close to the city, but estimated such a scenario to occur less than 1% of the time. His estimate was not far from our current estimates today. A more recent study by Heaton (1985), using a theoretical distribution of earthquakes in southern California, concluded that there could be more than a minute of warning for the larger, most damaging earthquakes. Here, we come to a similar conclusion using the set of past earthquakes in southern California and future likely earthquakes and existing seismic stations in northern California.

Active early warning systems are now operational in Mexico, Japan, Taiwan and Turkey (Espinosa Aranda et al. 1995; Wu et al. 1998; Wu and Teng 2002; Erdik et al. 2003; Odaka et al. 2003; Boese et al. 2004; Kamigaichi 2004; Nakamura 2004; Horiuchi et al. 2005; Wu and Kanamori 2005). Their warning messages are currently used by transportation systems such as rail and metro systems, as well as private industries, including construction, manufacturing and chemical plants. They are also used by utility companies to shut down generation plants and dams, and emergency response personnel to initiate action before ground shaking. In addition, schools receive the warnings allowing children to take cover beneath desks, housing units automatically switch off gas and open doors and windows, and entire complexes evacuate. Many of these applications would also be appropriate in California. WTPDF for the specific location of any user can be calculated and used to determine the cost-benefit of implementing an automated response to warning messages.

EWS are no panacea for the mitigation of seismic hazard. While EWS cannot warn everyone prior to all ground shaking events, they can offer warning to many affected people most of the time. No approach to natural hazard mitigation is perfect. Building codes are intended to prevent collapse of most structures in most earthquakes. If the mitigation of natural hazards is our intent, it is important to ensure that we continually ask what more could be done, what new technologies can be applied. As the De-

ember 26, 2004, tsunami disaster demonstrated most clearly, complacency is not an option.

### 3.6 Acknowledgments

This work benefited from discussions with Hiroo Kanamori, Yih-Min Wu, David Wald, Michael Brudzinski, and the seismic network operators of the CISN, in particular David Oppenheimer, Lind Gee, Douglas Neuhäuser and Egill Hauksson. Andrew Lockman, Erik Olson and Gilead Wurman contributed to the analysis. Support for this work was provided by the USGS National Earthquake Hazard Reduction Program and National Science Foundation.

### References

- Abrahamson NA, Silva WJ (1997) Empirical response spectral attenuation relations for shallow crustal earthquakes. *Seismo Res Lett* 68, 94-127
- Allen RM, Kanamori H (2003) The potential for earthquake early warning in Southern California. *Science* 300:786-789
- Boese M, Erdik M, Wenzel F (2004) Real-time prediction of ground motion from p-wave records. *Eos Trans AGU Fall Meet Suppl* 85, Abstract S21A.0251
- Bolt BA (1968) The focus of the 1906 California earthquake. *Bull Seismol Soc Am* 50:457-471
- Boore DM (1977) Strong-motion recordings of California earthquake of April 18, 1906. *Bull Seismol Soc Am* 67:561-577
- Boore DM, Joyner WB, Fumal TE (1997) Equations for estimating horizontal response spectra and peak acceleration from western North American earthquakes; a summary of recent work. *Seismo Res Lett* 68:128-153
- Campbell KW (1981) Near-source attenuation of peak horizontal acceleration. *Bulletin of the Seismological Society of America* 71:2039-2070
- Campbell KW (1997), Empirical near-source attenuation relationships for horizontal and vertical components of peak ground acceleration, peak ground velocity, and pseudo-absolute acceleration response spectra. *Seismo Res Lett* 68:154-179
- Cooper JD (1868) Earthquake indicator. In: *Evening Bulletin* (ed) San Francisco
- Erdik MO, Fahjan Y, Ozel O, Alcik H, Aydin M, Gul M (2003) Istanbul earthquake early warning and rapid response system. *Eos Trans AGU Fall Meet Suppl* 84, Abstract S42B.0153
- Espinosa Aranda JM, Jimenez A, Ibarrola G, Alcantar F, Aguilar A, Inostroza M, Maldonado S (1995) Mexico city seismic alert system. *Seismo Res Lett* 66:42-52

- Field EH (2000) A modified ground-motion attenuation relationship for southern California that accounts for detailed site classification and a basin-depth effect. *Bull Seismol Soc Am* 90:S209-S221
- Frankel A, Mueller C, Barnhard T, Perkins D, Leyendecker EV, Dickman N, Hanson S, Hopper M (1996) National seismic hazard maps. U.S. Geological Survey, Open-File Report 96-532, Denver
- Fukushima Y, Irikura K (1982) Attenuation characteristics of peak ground motions in the 1995 Hyogo-Ken. *J Phys Earth* 45:135-146
- Grasso VF, Allen RM (in review) Uncertainty in real-time earthquake hazard predictions
- Heaton TH (1985) A model for a seismic computerized alert network. *Science* 228:987-990
- Horiuchi S, Negishi H, Abe K, Kamimura A, Fujinawa Y (2005) An automatic processing system for broadcasting earthquake alarms. *Bull Seismol Soc Am* 95:708-718
- Joyner WB, Boore DM (1981) Peak horizontal acceleration and velocity from strong-motion records including records from the 1979 Imperial Valley, California, earthquake. *Bulletin of the Seismological Society of America* 71:2011-2038
- Kamigaichi O (2004) Jma earthquake early warning. *J Japan Assoc Earthquake Eng* 4
- Lockman A, Allen RM (2005) Single station earthquake characterization for early warning. *Bull Seism Soc Am* 95:2029-2039
- Lockman A, Allen RM (2007) Magnitude-period scaling relations for Japan and the Pacific Northwest: Implications for earthquake early warning. *Bull Seismol Soc Am*
- Lomax A (2005) A reanalysis of the hypocentral location and related observations for the great 1906 California earthquake. *Bull Seismol Soc Am* 95:861-877
- Nakamura Y (1988) On the urgent earthquake detection and alarm system (Uredas). *Proc. 9th World Conf. Earthquake Eng., VII*, 673-678
- Nakamura Y (1996) Real-time information systems for hazards mitigation. *Proceedings of Eleventh World Conference on Earthquake Engineering*, Paper No. 2134
- Nakamura Y (2004) Uredas, urgent earthquake detection and alarm system, now and future. *Proc. 13th World Conf. Earthquake Eng., August 2004*, Paper No. 908
- Odaka T, Ashiya K, Tsukada S, Sato S, Ohtake K, Nozaka D (2003) A new method of quickly estimating epicentral distance and magnitude from a single seismic record. *Bull Seismol Soc Am* 93:526-532
- Olson E, Allen RM (2005) The deterministic nature of earthquake rupture. *Nature* 438:212-215
- Richter CF (1958) *Elementary seismology*. W. H. Freeman, 768 pp
- Sadigh K, Chang CY, Egan JA, Makdisi F, Youngs RR (1997) Attenuation relationships for shallow crustal earthquakes based on California strong motion data. *Seismo Res Lett* 68:180-189

- Wald DJ, Quitoriano V, Heaton TH, Kanamori H (1999) Relationships between peak ground acceleration, peak ground velocity, and modified Mercalli intensity in California. *Earthquake Spectra* 15:557-564
- Wald DJ, Quitoriano V, Heaton TH, Kanamori H, Scrivner CW, Worden CB (1999) Trinet "shakemaps": Rapid generation of peak ground motion and intensity maps for earthquakes in Southern California. *Earthquake Spectra* 15:537-555
- Working Group on California Earthquake Probabilities (2003) Earthquake probabilities in the San Francisco Bay region: 2003 to 2031. U.S. Geological Survey
- Wu Y-M, Kanamori H (2005) Experiment on an onsite early warning method for the Taiwan early warning system. *Bull Seismol Soc Am* 95:347-353
- Wu Y-M, Kanamori H, Allen RM, Hauksson E (in review) An onsite earthquake early warning method for the Southern California seismic network. *Bull Seism Soc Am*
- Wu Y-M, Teng T-l (2002) A virtual subnetwork approach to earthquake early warning. *Bull Seismol Soc Am* 92:2008-2018
- Wu YM, Kanamori H (2005) Rapid assessment of damage potential of earthquakes in Taiwan from the beginning of p waves. *Bull Seism Soc Am* 95:1181-1185
- Wu YM, Shin TC, Tsai YB (1998) Quick and reliable determination of magnitude for seismic early warning. *Bull Seismol Soc Am* 88:1254-1259
- Zoback ML, Jachens RC, Olson JA (1999) Abrupt along-strike change in tectonic style: San Andreas fault zone, San Francisco Peninsula. *J Geophys Res* 104:10719-10742